ELSEVIER

Microelectronic Engineering 43–44 (1998) 325–333

MICROELECTRONIC ENGINEERING

Quantum wire splitting in nanostructures

Carsten Pigorsch[a,*], Wilfried Klix[b], Roland Stenzel[a]

[a]*Hochschule für Technik und Wirtschaft Dresden, Fachbereich Elektrotechnik, Friedrich-List-Platz 1, D-01069 Dresden, Germany*

[b]*Technische Universität Dresden, Institut für Grundlagen der Elektrotechnik/Elektronik, Mommsenstraße 13, D-01062 Dresden, Germany*

Abstract

The electron transport processes in novel semiconductor nanostructures are mainly influenced by quantum mechanical effects. Especially in heterostructures the effect of energy quantisation appears at the heterojunctions. This can be considered in device simulation by solving the Schrodinger equation in connection with the Poisson equation. In nanostructures the appearance of 1-dimensional or 2-dimensional electron gases is used for devices as current channels with a high electron mobility. The first systematic investigation of quantum wire structures is carried out to find the conditions for the creation of a real 1-dimensional electron gas as well as for the splitting of it into several electron gases at enlarged structure dimensions. A coupled microscopic/macroscopic algorithm is applied to simulate several nanometre quantum wire structures. The electron density in the quantum wire is calculated and compared for different shapes of the wire structure and for different material compounds and material dopings.

Keywords: Quantum wire; Novel heterojunction devices; Simulation; 1DEG

1. Introduction

One intention of modern semiconductor technology is the reduction of the device length and width. With the realization of these nanometre device sizes several quantum mechanical effects appear. The electrons and the holes can not move freely in the three spatial directions. The possible movement of the charge carriers is confined in one, two or all three directions, so that 2-, 1- or 0-dimensional electron gases arise. The self-consistent solution of the Poisson and Schrodinger equation is an accurate model to describe the quantum mechanical confinement and to compute the electron density distribution and the discrete electronic states.

In semiconductor heterostructures the confinement of the electron function appears at the heterojunctions because of the potential well and the potential barrier as a consequence of the conduction band discontinuity. In high electron mobility transistors a 2-dimensional electron gas (2DEG) is used as an active transistor channel. The 1DEG can be realized for instance in a V-grooved quantum wire where a non-planar substrate is overgrown by MBE [1].

*Corresponding author. Fax: +49-351-462 21 93; e-mail: pigorsch@et.htw-dresden.de

0167-9317/98/$19.00
PII: S0167-9317(98)00181-6

An efficient simulation model has been developed to compute these kinds of nanometre devices. One main problem in microscopic device simulation is the simulation time. To decrease this the microscopic model of Schrodinger and Poisson equation is applied only in the parts of the device where electron gases appear and is coupled with the known macroscopic drift–diffusion model for all other parts. The model is used to compute a test structure which is designed to investigate the occurrence of 1DEG in a quantum wire heterostructure and the splitting of the quantum wire in various 1DEG.

2. Model

For the simulation of compound semiconductor nanostructures a coupled microscopic/macroscopic algorithm has been developed and implemented [2]. The model includes the known macroscopic drift–diffusion model consisting of the Poisson equation and the transport and continuity equations for holes and electrons and the microscopic effective mass Schrodinger equation for electrons. The Schrodinger equation is solved only in the area where quantum mechanical effects are expected. In all of the other parts of the device structure the drift–diffusion model is applied. The Schrodinger equation is solved 1-dimensional or 2-dimensional according to the confinement of the electrons in the semiconductor structure.

The Schrodinger equation

$$-\frac{\hbar^2}{2}\nabla\cdot\left(\frac{1}{m^*}\nabla\psi\right)+(V-E)\psi=0 \tag{1}$$

and the Poisson equation

$$\nabla(\epsilon\cdot\nabla\varphi)=-q(p-n+N_D-N_A) \tag{2}$$

are solved self-consistently. m^* is the effective mass of the electrons and is assumed as a material constant. E represents the discrete energy levels, ψ represents the corresponding wavefunctions. $\hbar$ is the Planck constant. The potential energy V is defined as [3–6]

$$V=-q\varphi+\Delta E_C+E_{xc}+E_{im} \tag{3}$$

ΔE_C is the conduction band discontinuity at the heterojunction. The local exchange correlation potential energy E_{xc} and the image potential energy E_{im} are neglected at first because of their relative small value for the used material compounds [3].

The electrostatic potential is the result of the Poisson equation, the Schrodinger equation delivers the wavefunctions ψ_k of the calculated discrete energies E_k. The electron density is then

$$n=\sum_k n_k\cdot|\psi_k|^2+n_{bulk} \tag{4}$$

where n_k are the electron densities in the energy levels E_k [4,7]. These densities are calculated depending on the confinement of the electrons [8–10].

$$n_{k,2DEG}=\frac{m^*\cdot kT}{\pi\hbar^2}\ln\left[1+\exp\left(\frac{E_{Fn}-E_k}{kT}\right)\right] \tag{5}$$

$$n_{k,\mathrm{1DEG}} = \frac{\sqrt{2m^*kT}}{h} F_{-1/2}\left(\frac{E_{\mathrm{Fn}} - E_k}{kT}\right) \tag{6}$$

E_{Fn} is the quasi-Fermi energy of the electrons. The bulk electron density n_{bulk} is assumed in a 3D energy band above the discrete energy levels where the differences between adjoined levels are less than kT.

In another loop the transport equations

$$J_n = -q\mu_n n \cdot \nabla(\varphi + \Theta_n) + \mu_n \cdot kT \cdot \nabla n \tag{7}$$

$$J_p = -q\mu_p p \cdot \nabla(\varphi - \Theta_p) - \mu_p \cdot kT \cdot \nabla p \tag{8}$$

and the continuity equations

$$\nabla J_n = q \cdot \left(R - G + \frac{\partial n}{\partial t}\right) \tag{9}$$

$$\nabla J_p = -q \cdot \left(R - G + \frac{\partial p}{\partial t}\right) \tag{10}$$

for the electrons and the holes are solved, where R and G are the recombination and the generation rate, respectively.

The so called band parameters Θ_p and Θ_n, which are inserted in the transport equation to consider different materials in the device structure, are corrected so that the macroscopic Fermi–Dirac relation between the microscopic solution for the electron density and the solution for the electrostatic potential is preserved.

The calculation of the electron density as a function of the discrete energies and the wavefunctions requires the Fermi energy. The Fermi energy is determined by the solution of the electron density delivered from the transport equation.

3. Algorithm

The principle of the whole coupled microscopic/macroscopic algorithm is shown in Fig. 1. The iteration is initialized by the macroscopic solution of the drift–diffusion model. First the Fermi energy is calculated from the initial solution or the solution of the previous iteration step. The Fermi energy is constant during the following self-consistent solution of the Schrodinger and the Poisson equation. This delivers the microscopic electron density and the electrostatic potential. After that the electron density is changed by the solution of the macroscopic transport equation and the next step of the iteration starts.

The self-consistent solution in the inner loop is obtained, if the error tolerance of the potential and the electron density is reached. The outer loop of the algorithm with the transport equation is repeated until the electron density differs by less than a defined error.

In the algorithm the 1D Schrodinger equation can be solved at several discretization lines in a second direction and the 2D Schrodinger equation at several discretization planes in a third direction. These are called the quasi-2D and the quasi-3D solution, respectively. The calculation of the current

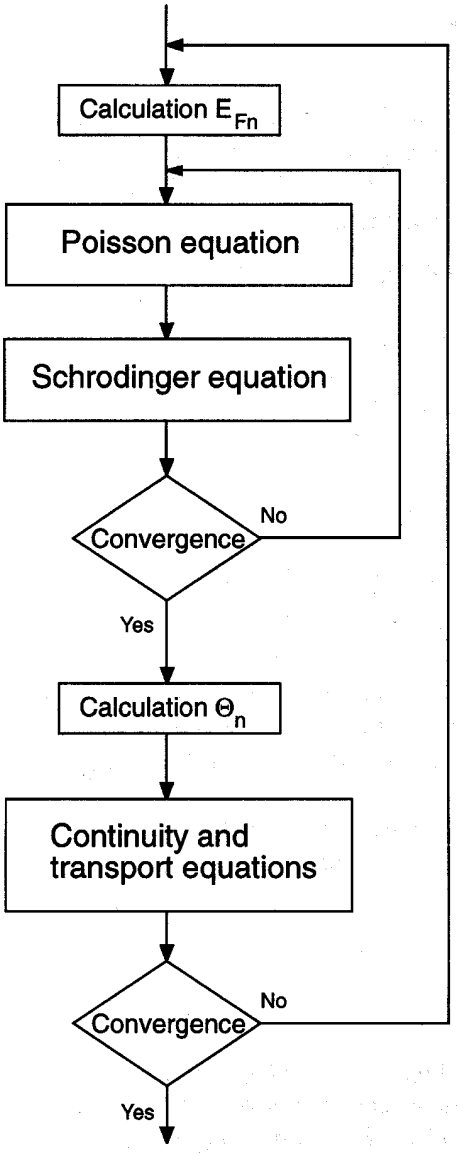

Fig. 1. Coupled microscopic/macroscopic simulation algorithm.

density in that direction by using the transport equation is possible if the differences between the eigenenergies of adjoining solutions are less than kT.

The Dirichlet boundary conditions are used for the Schrodinger equation. The electron density and so the occupation probabilities $|\psi_k|^2$ vanish on the boundaries. Therefore a region of electron-depletion should be the boundary of the device area where the Schrodinger equation is solved.

4. Numerical methods

The solution of the effective mass Schrodinger equation yields an eigenvalue problem. The eigenfunctions represent the wavefunctions, the eigenvalues are the subband energies.

For the transformation of the Schrodinger equation into the eigenvalue problem two methods are implemented: the Rayleigh–Ritz method (RRM) [10,11] and the finite differences method (FDM) [12]. The discretisation of the device area is done by a non-equidistant rectangular grid.

By using the RRM the wavefunctions are expressed as a sum of expansion functions in the form of

$$\psi(x) = \sum_i v_i(x) \quad 1 - \text{dimensional solution} \tag{11}$$

$$\psi(x,y) = \sum_i v_i(x) \sum_j w_j(y) \quad 2 - \text{dimensional solution} \tag{12}$$

where sine functions are applied to $v_i(x)$ and $w_j(y)$. The expansion functions have to be chosen in a way that the wavefunctions realize the boundary conditions. The result of the RRM is an eigenvalue problem with a symmetric coefficient matrix. The dimension of the matrix is equal to the number of expansion functions i or $i \cdot j$ and so it is independent of the discretization.

The FDM results in a band matrix and for the 1-dimensional solution of the Schrodinger equation in a tridiagonal matrix. This matrix can easily be transformed into a symmetric band matrix. The dimension of the eigenvalue problem is equal to the number of the discretization points.

The main differences between both methods are the resulting dimensions of the matrices and the band structure of the FDM-matrix in contrary to full RRM-matrix. This is taken into consideration for the solution method for the eigenvalue problem. Only a limited number of the lowest eigenvalues is required. The matrix has to be tridiagonalized and then the eigenvalues are calculated by the bisection algorithm and the Sturm sequence.

5. Results and discussion

To analyse the electron density and other electronic quantities in a quantum wire a test structure has been simulated as shown in Fig. 2. It consists of an undoped square GaAs-area with different edge-lengths surrounded with n-doped $Al_{0.3}Ga_{0.7}As$. The edge-length of the GaAs-area has been varied between 6 nm and 24 nm. The doping of the $Al_{0.3}Ga_{0.7}As$ is 10^{18} cm^{-3}. Because of the heterojunction and the small edge-length the electrons should be confined in a 1DEG. Fig. 3 represents the electron density distribution of the quantum wire with an edge-length of 6 nm in the thermodynamical equilibrium. The 1DEG arises with a maximum electron density in the centre of the GaAs-area. If the edge-length is increased to 24 nm the quantum wire is split into four single 1DEG (Fig. 4). The electron density has four maxima near the corners of the GaAs-area. At the heterojunctions between the GaAs and the $Al_{0.3}Ga_{0.7}As$ 2-dimensional electron gases arise.

The quantum wire splitting depending on the edge-length is compared in Fig. 5. There an intersection of the electron density diagonal through the squared GaAs-region (see Fig. 2) for different

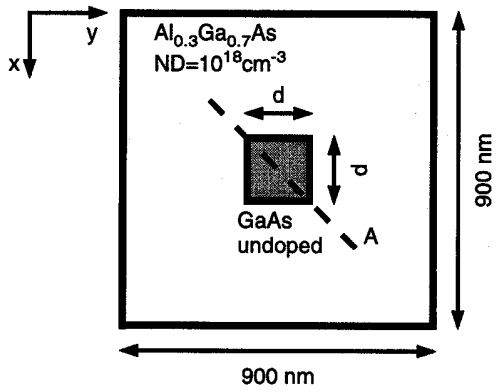

Fig. 2. Quantum wire test structure. Edge-length d and intersection line A.

lengths is plotted. The maxima of the density in the 1DEG decreases with an enlarged edge-length and the distance between them grows larger.

The resistances of these quantum wires calculated for a voltage of 70 mV and a wire length of 1.6 μm are represented in Fig. 6. A linear dependence appears between the resistance and the cross-section for the wires with the larger edge-lengths and the split electron gas. If the quantum wire consists of only one 1DEG the resistance increases heavily. A resistance of 8 kΩ/μm appears for the 6 nm structure. Because of this large resistance the current through such an quantum wire has to be limited to avoid a large voltage drop in nanoelectronic devices.

Other simulations were carried out to compare the electron gas in the structure for different dopings of the $Al_{0.3}Ga_{0.7}As$ and for another material compound. A higher doping concentration in the $Al_{0.3}Ga_{0.7}As$ of 5×10^{18} cm^{-3} and 10^{19} cm^{-3} yields an adequate higher number of electrons in the

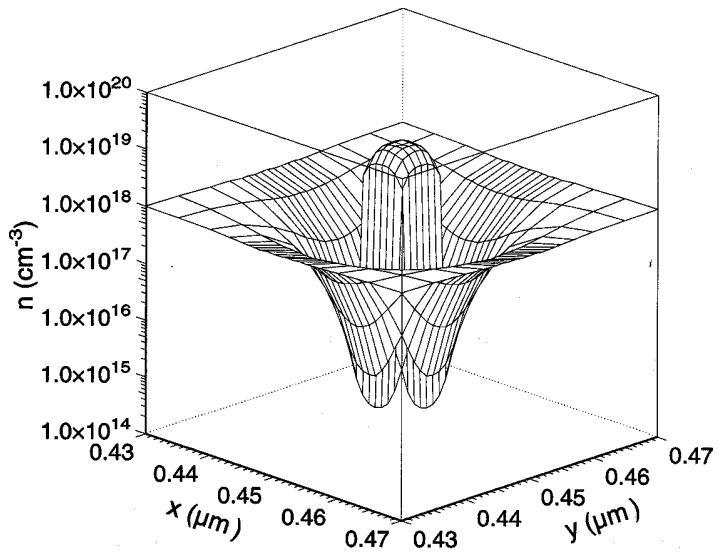

Fig. 3. Electron density of a quantum wire with edge-length of 6 nm.

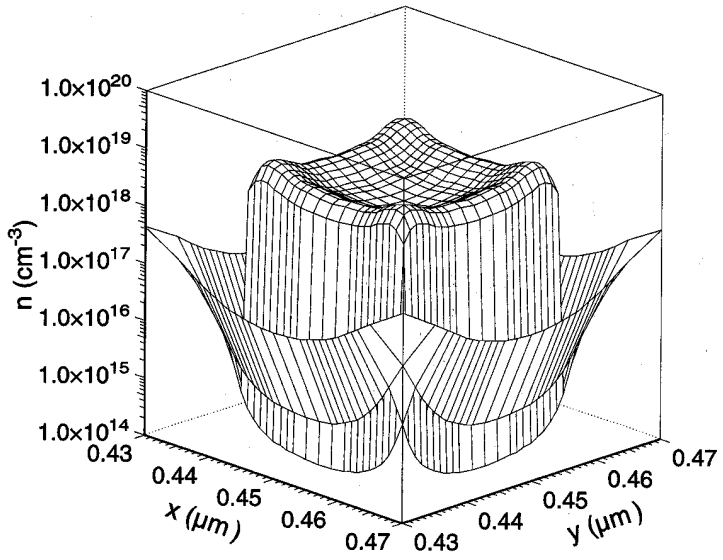

Fig. 4. Electron density of a quantum wire with edge-length of 24 nm.

quantum wire and a higher maximum of the electron density. The potential well at the heterojunctions is narrower and so the splitting of the quantum wire already appears in the 6 nm wire structure. The same effect arises for the material compound of $In_{0.53}Ga_{0.47}As$ surrounded by $Al_{0.48}In_{0.52}As$. Here the

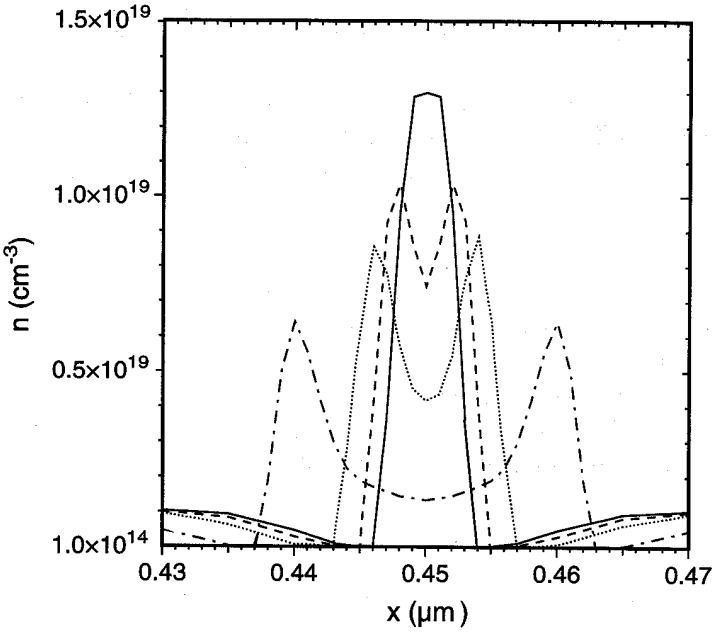

Fig. 5. Electron density of the quantum wires with different edge-lengths (intersection line *A*). Solid line: $d=6$ nm, dashed line: $d=8$ nm, dotted line: $d=12$ nm, dot–dashed line: $d=24$ nm.

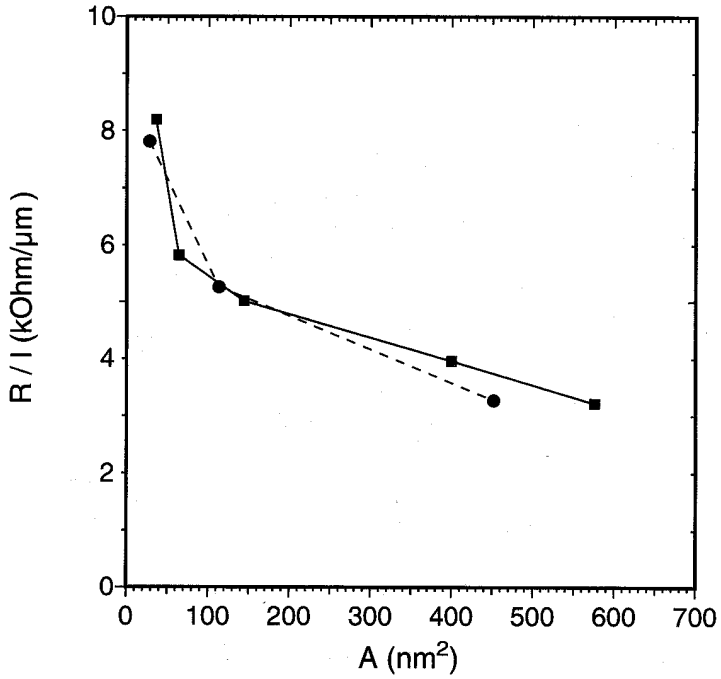

Fig. 6. Cross-section dependence of the resistence per length of the quantum wire. Square-marked: squared cross-section, circle-marked: circular cross-section.

conduction band discontinuity ΔE_C is 550 meV compared with a discontinuity of 330 meV in the $GaAs/Al_{0.3}Ga_{0.7}As$ structure.

Additionally, the electron densities in a quantum wire of a circular GaAs-area are computed. For a diameter of 6 nm again a 1DEG occurs. If the diameter is increased to 24 nm the wire consists of a 2DEG along the heterojunction. Because of the absent corners in the structure there is no real 1DEG.

6. Conclusion

A coupled microscopic/macroscopic simulation algorithm has been presented. It includes the solution of the 1D and the 2D Schrodinger equation. An efficient solver for this differential equation and the corresponding eigenvalue problem has been implemented. Several simulations regarding a quantum wire test structure have been represented. In this structure a single 1DEG occurs only for a very small edge-length of 6 nm. In most of the other cases 2DEG arise at the heterojunctions which bound the 1DEG at the corners of the wire structure.

References

[1] F. Rossi, E. Molinari, R. Rinaldi, R. Cingolani, Solid-St. El. 40 (1996) 249–255.
[2] C. Pigorsch, R. Stenzel, W. Klix, SISDEP, Vol. 6, Springer 1995, pp. 230–233.

[3] S.E. Laux, Proc. of NASECODE V, Dublin, 1987, Boole Press Lim., pp. 270–275.
[4] T. Wang, C.-H. Hsieh, IEEE Trans. ED 37 (1990) 1930–1938.
[5] T. Kerkhoven, A.T. Galick, U. Ravaioli, J.H. Arends, Y. Saad, J. Appl. Phys. 68 (1990) 3461–3469.
[6] F. Stern, S.D. Sarma, Phys. Rev. 30 (1984) 840–848.
[7] S.-H. Ng, R. Khoie, R. Venkat, IEEE Trans. ED 38 (1991) 852–861.
[8] D. Delagebeaudeuf, N.T. Linh, IEEE Trans. ED 29 (1982) 955–960.
[9] S.E. Laux, A.C. Warren, IEDM 1986, pp. 567–570.
[10] A. Abou-Elnour, K. Schuenemann, Sol.-State El. 37 (1994) 1817–1824.
[11] S.H. Gould, Variational Methods for Eigenvalue Problems, 2nd ed., Toronto, Ont. Canada, Univ. of Toronto Press, 1957.
[12] I.-H. Tan, G.L. Snider, L.D. Chang, E.L. Hu, J. Appl. Phys. 68 (1990) 4071–4076.